Sub Topic: Laminar Flames

10th U. S. National Combustion Meeting
Organized by the Eastern States Section of the Combustion Institute
April 23-26, 2017
College Park, Maryland

Flame temperature effect on the transition between soot and graphitic carbon products in premixed stagnation flames

*Jonathan Bonpua and Joaquin Camacho**

Mechanical Engineering Department, San Diego State University, USA
**Corresponding Author Email: jcamacho@sdsu.edu*

Abstract: Particulate carbon is known to exist in a wide range of forms, some of which exhibit properties that are desirable for emerging technologies. For example, graphitic carbon is widely integrated into energy storage devices due to its charge storage capacity and inherent electrical conductivity. The effect of flame temperature on the structure of carbon products formed in premixed stagnation flames is assessed in this work. Namely, the progression of carbon products from amorphous soot to more ordered carbon structures is examined by tracking the evolution of X-ray diffraction patterns and Raman spectra as a function of flame temperature and other flame parameters. The stagnation flames are modeled in a pseudo-1D formulation to precisely quantify the temperature-time relationship in the carbon growth region. No crystalline structure was observed for deposited films from the 1826 and 2032 K flames as evidenced by the broad amorphous peak at low 2theta. Similarly, the Raman spectra for the flame-formed carbon only showed prominent peaks representing the D and G band close to 1350 and 1600 cm-1, respectively. A slight increase in D band intensity is observed in the 2032 K flame relative to the 1826 K flame. Higher temperatures will be accessed to determine whether graphitic carbon properties could be achieved in flame-synthesized products in future work. The observations made here provide insight into carbon formation in flames that is useful for soot theory / modeling and flame synthesis processes.

Keywords: Flame Synthesis, Carbon, Nanoparticle, Soot

1. Introduction

Besides being a problematic by-product of combustion processes, carbon, in its many forms, can also be the desired end-product from flames. There are similarities between nuisance soot and more useful graphititc forms of carbon. These similarities have been invoked to describe soot reactivity by referring to experiments [1] on graphite. In addition, soot growth and ageing is regularly described by the degree of graphitization in the carbon structure. Dobbins and co-workers [2, 3] were the first to draw upon classical works on carbonization (see e.g., [4, 5]) to describe the evolution of so-called precursor particles (also known as nascent soot in more recent works [6-8]) to mature soot. For producing useful carbon materials, relatively high flame temperatures are important for achieving carbonization and uniform growth conditions are necessary to obtain precisely controlled properties. The essential commodity known as carbon black is produced industrially using flames operating at the aforementioned conditions.

In this work, the range of flame conditions leading to less-desirable soot formation and more valuable graphitic carbon will be demonstrated. Stretch-stabilized premixed flames will be used because the stabilization mechanism allows for a pseudo one-dimensional flame without

significant heat loss [9]. These flame characteristics will enable particle formation under uniform growth conditions with temperatures approaching 2500K. Raman Spectroscopy and X-ray diffraction (XRD) will serve as diagnostics for the presence of sp^2 bonded carbon and degree of crystallinity, respectively. The raman spectra of amorphous, crystalline and nano-scale carbon have been extensively studied. Soot structural details have also been investigated in raman spectroscopy studies [7, 10-14]. Boehman and co-workers incorporated analysis of the Raman spectra for laboratory [13] and Diesel engine [14] soot to examine soot reactivity and carbon structure. Russo and Ciajolo carried out a systematic Raman study on soot from premixed flames and parsed out subtle differences in soot structure resulting from fuel structure and flame conditions [12].

Empirical [15] and theoretical [16] works showing the relationship between XRD derived crystallite size and the ratio of prominent bands in the Raman spectra marked the beginning of numerous XRD and Raman studies as complimentary carbon diagnostics. XRD peaks attributed to (002), (10) and (110) have been reported for both soot and carbon black [14]. Graphite and turbostratic carbon are known to have one major XRD peak attributed to (002) [17]. In this work, complimentary XRD and Raman analysis will be carried out to isolate the effect of flame temperature on the carbon products formed in premixed flames. The relatively high-temperature that is accessible in premixed stretch-stabilized flames is expected to allow for observation of higher ordered carbon structure relative to carbon products obtained at lower flame temperatures.

2. Experimental

The experimental setup, summarized in Fig. 1, consists of a burner with an aerodynamically shaped nozzle and a stagnation / deposition surface. The stabilization mechanism of the premixed flames studied herein requires flow stagnation to set the kinematic balance between the local flame speed and normal flow velocity immediately upstream of the flame surface [9]. As such, a water-cooled aluminum stagnation surface is held at a distance, L, of 1.0 cm from the burner nozzle. Microscope slides were placed flush with the surface for deposition of carbon aerosol formed in the flame. The aerodynamic shape of the burner nozzle body is designed to achieve plug flow at the burner exit (1.43 cm nozzle exit diameter). The standing distance between the flame and stagnation / deposition surface, L_s, may be varied by changing the unburned gas flow rate. The gas temperature at the nozzle exit, T_n, was measured with an uncoated fine-wire (125 μm wire diameter) Pt-Rh thermocouple placed near the centerline of the flow. The temperature at the stagnation surface, T_s, was measured by a type-K thermocouple (0.2 cm wire diameter). The gas temperature at the nozzle exit was determined to be T_n = 340 K; and the stagnation surface temperature was T_s = 385 K. Numerical sensitivity calculations show that within the uncertainty values quoted the flame structure exhibits little sensitivity towards the boundary temperature variations.

The carbon structure of the flame products was analyzed by XRD and Raman spectroscopy for a series of premixed ethylene flames. The flame diluent was alternated between nitrogen and argon to expand the range of acceptable flame temperatures. The unburned gas composition and cold gas velocity are summarized in Table 1 for each flame. The maximum flame temperatures computed using OPPDIF and USC Mech II (to be discussed later) are around 1830 and 2030 K. In each series, the variation in unburned gas velocity has the effect of changing the flame

standoff distance by altering the kinematic balance between the local flame speed and the normal flow velocity immediately upstream of the flame surface [9]. The examined flames range from relatively high velocity flames approaching the limit where stretch-induced flame extinction processes occur to low velocity flames approaching the flashback limit. The expected size of the carbon products is 20 nm and below based on a previous study examining the evolution of soot particle size distribution [Camacho 2015] under similar flame conditions.

A modified OPPDIF computation [18] based on USC Mech II [19] was used to calculate the temperature, velocity and species profiles. The boundary conditions were given by the measured temperatures at the nozzle exit and the stagnation surface/sampling probe. The OPPDIF code invokes the pseudo one-dimensional formulation introduced by Kee, Smooke and co-workers [20, 21]. Plug flow is designated at the burner boundary and non-slip conditions are assumed at the stagnation surface boundary. For particles formed in the flame, the finite residence time is determined by considering the thermophoretic velocity which is driven by the significant temperature gradient, $\partial T/\partial x$, at the stagnation plate. The thermophoretic velocity was calculated numerically and added to the total velocity. The residence time of the soot particles is defined as the time interval for the particle (or precursors) to traverse from the calculated location of the peak flame temperature to the location of the stagnation probe.

The carbon flame products were analyzed by X-ray diffraction (XRD) and Raman Spectroscopy. XRD measurements were carried out on microscope slides upon which the film was directly deposited. A PANalytical X'pert Pro diffractometer was used with a Cu X-ray tube operating at 45 kV and 40 mA. The beam was conditioned by an X-ray mirror and a Ni beam attenuator. The diffracted beam is collected with a parallel plate collimator and a proportional photon detector. Diffraction patterns were obtained at 0.05 degrees per step and 1 second per step for films from both precursor loadings. For Raman spectroscopy, a Thermo Nicolet DXR Raman Microscope (Thermo Scientific) with a 532 nm laser was used. The laser power was 5 mW and changes to the spectra and sample occurred over the sampling period.

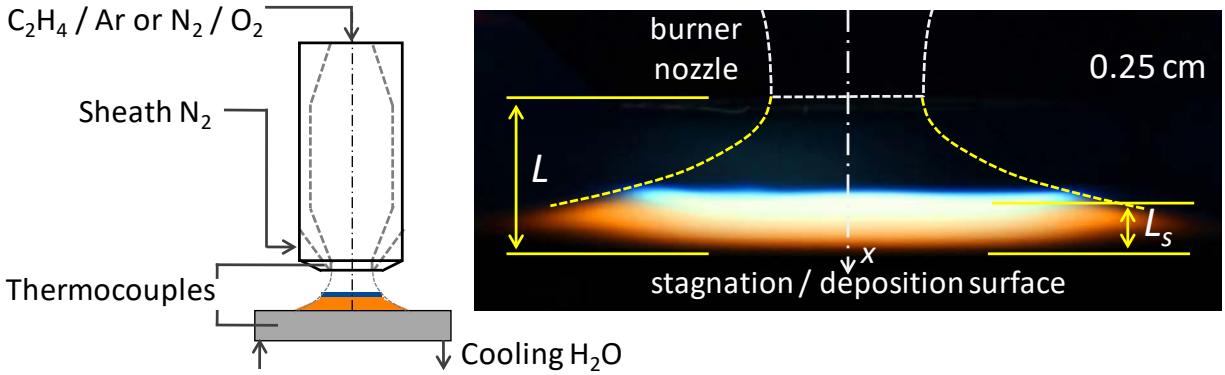

Figure 1: Experimental setup for carbon synthesis and deposition in premixed stagnation flames.

3. Results and Discussion

Particles formed in the flame deposited onto a glass microscope slide and formed a porous film. XRD patterns of the as-deposited films are shown in Fig. 2. No crystalline structure was

observed for deposited films from the 1826 and 2032 K flames as evidenced by the broad amorphous peak at low 2theta. As a reference, the Raman spectra of highly ordered pyrolytic graphite was measured and the expected G band peak is prominent. The Raman spectra for the flame-formed carbon only showed prominent peaks representing the D and G band close to 1350 and 1600 cm^{-1}, respectively. A slight increase in D band intensity is observed in the 2032 K flame relative to the 1826 K flame. The relative intensity of these bands has been attributed to the change in aromatic layer size [15] and the area of aromatic domains [22].

Table 1. Flame parameters[a]

Velocity, v_0 (cm/s)	Standing distance, L_s (cm)	Time, $t_p(L)$ (ms)	$T_{f,max}$ (K)
15.0% C_2H_4/18.5% O_2/66.5% N_2 (T_{ad} = 1805 K)			
20.2	0.53	17	1826
17.6% C_2H_4/22.2% O_2/60.2% Ar (T_{ad} = 2005 K)			
30.3	0.71	9	2032

[a] All unburned mixtures have the equivalence ratio equal to 2.4. Nozzle-to-stagnation surface separation (L) is 1 cm. [b] Unburned gas velocity at 298K and 1 atm. Sheath N_2 velocity is v_o. [c] Distance from the stagnation surface to position of maximum flame temperature. [d] Computed using OPPDIF and USC Mech II with T_n = 343 K and T_s = 395 K.

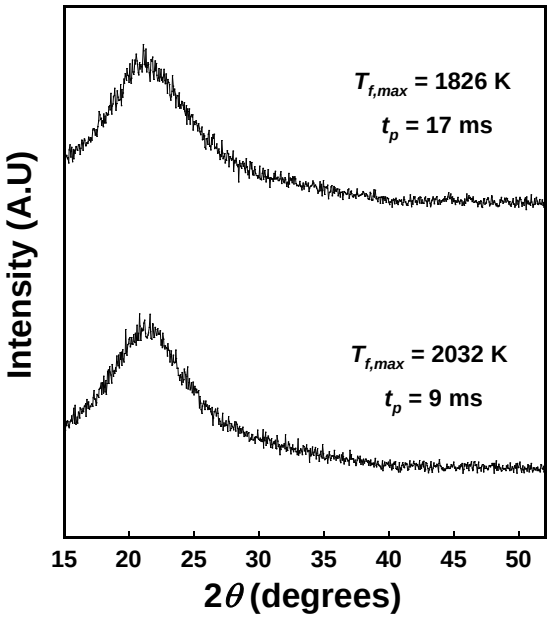

Figure 2: XRD patterns of as-deposited carbon films

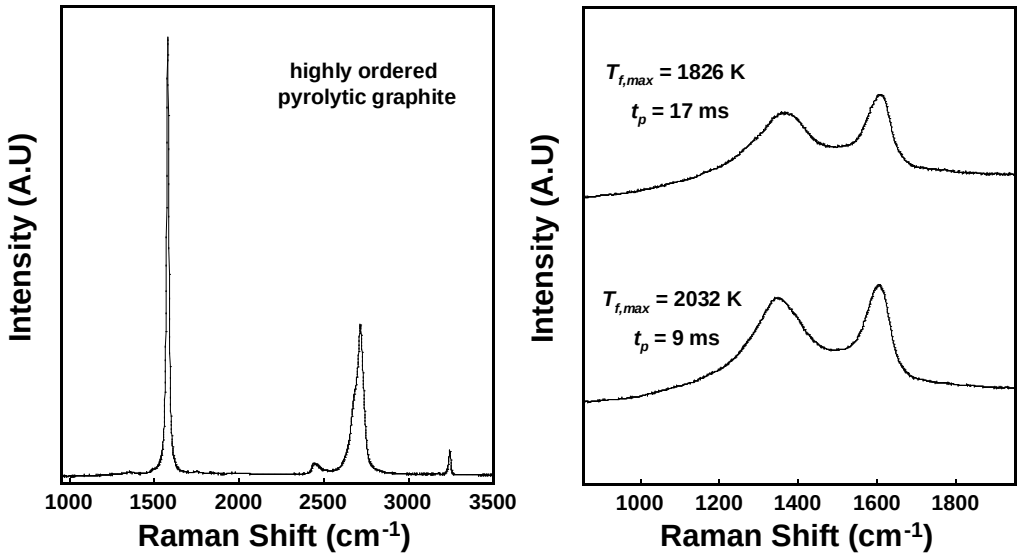

Figure 3: Raman spectra of highly ordered pyrolytic graphite (left) and as-deposited carbon films

4. Conclusion

No crystalline structure was observed for deposited films from the 1826 and 2032 K flames as evidenced by the broad amorphous peak at low 2theta. Similarly, the Raman spectra for the flame-formed carbon only showed prominent peaks representing the D and G band close to 1350 and 1600 cm^{-1}, respectively. A slight increase in D band intensity is observed in the 2032 K flame relative to the 1826 K flame. Higher temperatures will be accessed to determine whether graphitic carbon properties could be achieved in flame-synthesized products.

5. Acknowledgements

The work was supported by the University Grants Program at San Diego State University. The authors are thankful to Prof. David Pullman and Joan Kimbrough for generous access and help with Raman and XRD analysis, respectively.

6. References

[1] Walls JR, Strickland-Constable RF. Oxidation of carbon between 1000 and 2400 °C. Carbon 1 (1964) 333-334.
[2] Dobbins RA, Govatzidakis GJ, Lu W, Schwartzman AF, Fletcher RA. Carbonization Rate of Soot Precursor Particles. Combust. Sci Tech. 121 (1996) 103.
[3] Dobbins RA. Soot inception temperature and the carbonization rate of precursor particles. Combust. Flame 130 (2002) 204.
[4] Lewis IC. Chemistry of carbonization. Carbon 20 (1982) 519.
[5] Franklin R. The structure of graphitic carbons. Acta Crystall. 4 (1951) 253.
[6] Wang H. Formation of nascent soot and other condensed-phase materials in flames. Proc. Combust. Inst. 33 (2011) 41.

[7] Herdman JD, Connelly BC, Smooke MD, Long MB, Miller JH. A comparison of Raman signatures and laser-induced incandescence with direct numerical simulation of soot growth in non-premixed ethylene/air flames. Carbon 49 (2011) 5298.
[8] Kholghy MR, Veshkini A, Thomson MJ. The core-shell internal nanostructure of soot: A criterion to model soot maturity. Carbon 100 (2016) 508.
[9] Law CK. Combustion Physics. Cambridge: Cambrige Press, 2006.
[10] Lapuerta M, Oliva F, Agudelo JR, Stitt JP. Optimization of Raman Spectroscopy Parameters for Characterizing Soot from Different Diesel Fuels. Combust. Sci Tech. 183 (2011) 1203.
[11] Sadezky A, Muckenhuber H, Grothe H, Niessner R, Paschl U. Raman microspectroscopy of soot and related carbonaceous materials: Spectral analysis and structural information. Carbon 43 (2005) 1731.
[12] Russo C, Ciajolo A. Effect of the flame environment on soot nanostructure inferred by Raman spectroscopy at different excitation wavelengths. Combust. Flame 162 (2015) 2431.
[13] Seong HJ, Boehman AL. Studies of soot oxidative reactivity using a diffusion flame burner. Combust. Flame 159 (2012) 1864.
[14] Seong HJ, Boehman AL. Evaluation of Raman Parameters Using Visible Raman Microscopy for Soot Oxidative Reactivity. Energy Fuel 27 (2013) 1613.
[15] Tuinstra F, Koenig JL. Raman Spectrum of Graphite. J. Chem. Phys. 53 (1970) 1126.
[16] Lespade P, Al-Jishi R, Dresselhaus MS. Model for Raman scattering from incompletely graphitized carbons. Carbon 20 (1982) 427.
[17] Li ZQ, Lu CJ, Xia ZP, Zhou Y, Luo Z. X-ray diffraction patterns of graphite and turbostratic carbon. Carbon 45 (2007) 1686.
[18] Abid AD, Camacho J, Sheen DA, Wang H. Quantitative measurement of soot particle size distribution in premixed flames: The burner-stabilized stagnation flame approach. Combust. Flame 156 (2009) 1862.
[19] Wang H, You X, Joshi AV, Davis SG, Laskin A, Egolfopoulos F, Law CK. USC Mech II. High-Temperature Combustion Reaction Model of H2/CO/C1-C4 Compounds. http://ignis.usc.edu/USC_Mech_II.htm 2007.
[20] Kee RJ, Miller JA, Evans GH, Dixon-Lewis G. A computational model of the structure and extinction of strained, opposed flow, premixed methane-air flames. Symp. (Int.) Combust. 22 (1989) 1479.
[21] Lutz AE, Kee RJ, Grcar JF, Rupley FM. OPPDIF: A Fortan program for computing opposed-flow diffusion flames. Livermore: Sandia National Labs, 1997.
[22] Ferrari AC, Robertson J. Interpretation of Raman spectra of disordered and amorphous carbon. Phys. Rev. B 61 (2000) 14095.